Non-Arrhenius response of glass-forming liquids

R. V. Chamberlin
Department of Physics and Astronomy, Arizona State University, Tempe, Arizona 85287-1504
(Received 17 December 1992; revised manuscript received 23 July 1993)

A Gaussian size distribution of independently relaxing domains is used to model the response of various glass-forming liquids. With a single temperature-dependent parameter, the model accurately characterizes the observed dielectric susceptibility of salol and glycerol [P. K. Dixon *et al.*, Phys. Rev. Lett. **65**, 1108 (1990); N. Menon *et al.*, J. Non-Cryst. Solids **141**, 61 (1992)] over more than 13 orders of magnitude in frequency. The quality and range of these data allow quantitative confirmation of all assumptions of the model. As a function of temperature, the model gives excellent agreement with observed asymptotic relaxation rates (w_∞) via $[\ln(1/w_\infty)-\ln(1/w_0)] \propto \bar{s}$, where $\bar{s}$ is a temperature-dependent average domain size, and w_0 a *constant* intrinsic relaxation rate. Thus, the model provides a physical explanation for non-Arrhenius primary response, without resorting to the three adjustable parameters of the Vogel-Tammann-Fulcher law.

INTRODUCTION

Few materials obey Arrhenius' law for dynamical response.[1,2] The most commonly used empirical expression for the temperature (T) dependence of the peak absorption frequency (ν_p) is the Vogel-Tammann-Fulcher[3–5] (VTF) law $[\ln(1/\nu_p)-\ln(1/\nu_0)] \propto 1/(T-T_0)$, where ν_0 and T_0 are constants, and $T_0 > 0$ indicates deviation from Arrhenius behavior. Although the VTF law has been used to characterize response from a wide variety of materials, its specific temperature dependence is difficult to justify using conventional modifications of Arrhenius' law.[6] Furthermore, measurements over a sufficient range invariably show deviations from VTF behavior,[7] indicating that the VTF law is only an approximation. Other expressions have been proposed,[8–11] but most have at least three adjustable parameters, and none is clearly favored over the VTF law. The Williams-Landel-Ferry expression is a variation of the VTF law in which $T-T_0$ is replaced by free volume.[12,13] This modification has theoretical justification,[14] but usually does not fit data as well as the VTF law.[6] A key feature of the free-volume approach is that net response comes from coherent clusters, which relax via activation over potential barriers with heights that *increase* with increasing cluster size, so that non-Arrhenius behavior arises from a temperature-dependent average cluster size.[15] The principal distinction of our approach is that we consider the relaxation of low-energy, internal degrees of freedom, for which the energy-level spacing *decreases* with increasing size. Our approach is an example of localized normal-mode analysis, similar to that first proposed by Zwanzig,[16] but differs from most recent treatments[17] which neglect the size-dependence of the relaxation rate.

Generally, systems that exhibit non-Arrhenius temperature dependence also exhibit non exponential relaxation.[2,18] Common empirical expressions that have been used to characterize the observed response from a wide variety of materials include the Kohlrausch-Williams-Watts (KWW) stretched exponential $e^{-(t/\tau)^\beta}$, Curie-von Schweidler powerlaw $t^{-\alpha}$, and Néel logarithmic time dependence $\ln(t)$.[19,20] Unfortunately, these mathematical functions are also common approximations to a wide variety of models,[21] hence fitting with these functions cannot isolate a specific mechanism. Furthermore, all of these functions have divergent slopes at short times, hence they can only be approximations valid over a limited range. Indeed, measurements over sufficient range invariably demonstrate deviations from these expressions. Recently a specific model has been shown to provide better agreement with the observed response from dozens of different materials, including magnetic relaxation in spin glasses, oxide superconductors, and single-crystal ferromagnets;[22–25] structural relaxation in liquids, glasses, polymers, and crystals;[25–28] as well as dielectric susceptibility of glass-forming liquids.[27,28] Here we show that this model provides a physical explanation for temperature-dependent relaxation rates, and excellent agreement with observed non-Arrhenius response of glass-forming liquids, without resorting to the three adjustable parameters of the VTF law.

MESOSCOPIC MODEL

Our model is based on the assumption that a macroscopic sample contains a myriad of independently relaxing regions. We define a dynamically correlated domain (DCD) as a region where excitations relax with a single (locally uniform) relaxation rate. In some systems, a DCD may correspond to a region where local excitations share a common phase factor (quantum mechanically coherent), thus ensuring uniform relaxation throughout the domain. Thermodynamically, a DCD is a locally canonical system, whose energy need not be in equilibrium with neighboring domains or the thermal bath. The prevalence of inhomogeneous spectral broadening indicates that many amorphous materials possess a distribution of local relaxation rates.[29] Time- and temperature-

dependent magnetizations of EuS (Ref. 23) and Fe (Ref. 24) show that DCD's can dominate the behavior of ordered single crystals. Multidimensional NMR has clearly demonstrated that the primary response in a glass-forming liquid is due to a heterogeneous distribution of DCD's, which become dynamically homogeneous only after essentially all of the primary response is complete;[30] a typical average diameter is found to be ~ 35 Å.[31]

A simple picture of correlated vibrations (phonons) is as follows. (Similar pictures apply to magnons, polaritons, etc.) In condensed matter at finite temperatures, molecules may execute random (Einstein-oscillator-like) local vibrations. A reduction in energy occurs if neighboring particles fluctuate coherently, so that they maintain virtually equilibrium separation at all times, not merely when time averaged. Since this energy reduction is on the order of $k_B T$, these "dynamical correlations" will be thermally distributed throughout the sample, and may influence behavior at all temperatures. For harmonic interactions in a perfect crystal, Bloch's theorem requires that all fluctuations be a linear combination of plane-wave excitations; in real systems, normal-mode excitations may be transiently localized into DCD's. Many physical systems exhibit evidence for mesoscopic dynamic correlation,[32–34] including the simulated two-dimensional liquid shown in Fig. 1.[35] In Fig. 1, distinct dots indicate "molecules" that oscillate harmonically about an equilibrium position, whereas snakelike chains indicate diffusive motion characteristic of a boundary between dynamically correlated domains.

Assuming a domain-size distribution n_s, with size-dependent initial response P_s and relaxation rate w_s, the net relaxation is the weighted sum over all sizes

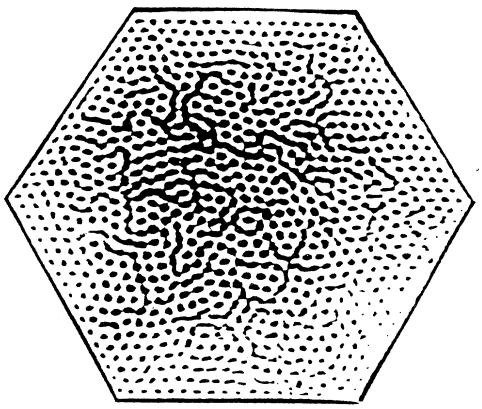

FIG. 1. Analog simulation of a two-dimensional liquid (Ref. 35). Steel balls, 1/16 in. in diameter, are placed between two electrified conducting plates, so that the balls experience repulsive dipolar interaction. The apparatus is placed on a vibration table to simulate temperature. Raw video images (~ 30 frames/sec) appear to show random "molecular" vibration. This photograph was made using a 1-sec exposure time, from video images averaged over 16 frames. Video averaging suppresses harmonic oscillations, revealing blurred (snakelike) surfaces of diffusive motion, which form boundaries between dynamically correlated domains.

$P(t)=\sum_{s=0}^{\infty}[P_s n_s]e^{-tw_s}$. Here s is the number of particles in a DCD, which contribute to response, hence s is usually proportional to volume. Some physically reasonable assumptions are made to obtain the size dependences of P_s, n_s, and w_s.

Equilibrium response is assumed to be proportional to the number of responding particles, $P_s=P_0 s$, which is simply the thermodynamic requirement that response per particle (P_0) is a homogeneously intensive quantity. If a system is to approach thermodynamic equilibrium, detailed balance requires that the ratio of relaxation rates between states separated by energy δE_s must be $e^{-\delta E_s/k_B T}$;[36] thus, assuming a uniform asymptotic rate (w_∞), local relaxations obey activated (Arrhenius-like) behavior, $w_s=w_\infty e^{-\delta E_s/2k_B T}$. The key assumption which distinguishes our approach is that we consider the relaxation of low-energy internal-degrees of freedom, for which the density of states is proportional to volume $\delta N/|\delta E_s| \propto s$, so that the spacing between adjacent ($\delta N=1$) energy levels is $|\delta E_s| \propto 1/s$.[37] In 1937, Fröhlich[38] first considered finite-size effects in perfect spheres, and obtained the standard quantum-mechanical result that energy levels vary inversely proportional to radius squared, $|\delta E_s| \propto 1/s^{2/3}$. In 1962, Kubo[39] recognized that imperfections will normally remove the degeneracies inherent in ideal spheres, so that real mesoscopic systems usually obey the thermodynamic requirement: $|\delta E_s| \propto 1/s$. We implement this requirement to obtain relaxation rates that vary exponentially with inverse size.

This key assumption, that densities of states are extensive quantities, can be pictured in several ways. For simple comparison to local excitations (Fig. 2), consider a one-dimensional lattice of alternating masses m_1 and m_2, connected by springs of constant κ.[40] Initially let $m_2=\infty$ [Fig. 2(a)], so that motion consists of local (Einstein) oscillators with degenerate energy $E_1=\hbar\sqrt{2\kappa/m_1}$. Even if randomness removes the degeneracies, local oscillations do not depends on domain size. For finite m_2 [Figs. 2(b) and 2(c)] interactions between local oscillators yield dispersive phonon bands. In general, bandwidths ($\Delta\sim\hbar\sqrt{\kappa/m_{1,2}}$) are independent of domain size, whereas the number of degrees of freedom that fill the bandwidth is proportional to s; hence the *average* energy-level spacing is $|\delta E_s| \propto 1/s$.

Figure 3 is a comparison to the picture that slow relaxation comes from activation of statically correlated clusters. Often, potential energy is plotted as a function of configuration, where nearby points in configuration space represent small changes in the positions of a few atoms.[41] Slow relaxation is attributed to activation over large barriers (involving sudden repositioning of many particles) to a distant configuration, Fig. 3(a). Such a picture requires considerable structural inhomogeneity (large rigid clusters held softly in place) and immediate communication across the sample (if the system is to be defined by a single configuration space). Often, barrier heights are assumed to increase with some power-law size dependence, $|\delta E_s| \propto s^\alpha$; generally, large rigid clusters have large barriers, so that $\alpha>0$. By contrast, we consider internal de-

grees of freedom governed by thermodynamics, so that $\alpha=-1$; energy-level spacings decease with increasing size because large domains have more degrees of freedom. Furthermore, DCD formation does not require *structural* inhomogeneity, and during primary response, communication occurs only across mesoscopic regions of the sample. [Secondary responses that involve communication between domains (e.g. domain growth, direct energy exchange, or particle diffusion) are assumed to occur after primary response, as shown by multidimensional NMR.[30]] To relate our picture to the previous view, consider a local configuration space for each DCD, Fig. 3(b). Since DCD's are finite sized, each configuration space is discretized, so that energy-levels near a local minimum may resemble a quantized oscillator. Primary response involves changing the level of excitation about distinct local minima. Slow relaxation comes from a rapid intrinsic attempt frequency, which is reduced by the virtually balanced net relaxation rate between closely spaced energy levels. Thermodynamics requires that the density-of-states of all dispersive excitations must be proportional to the volume of their domain, hence the average energy-level spacing is $|\delta E_s| \propto 1/s$.

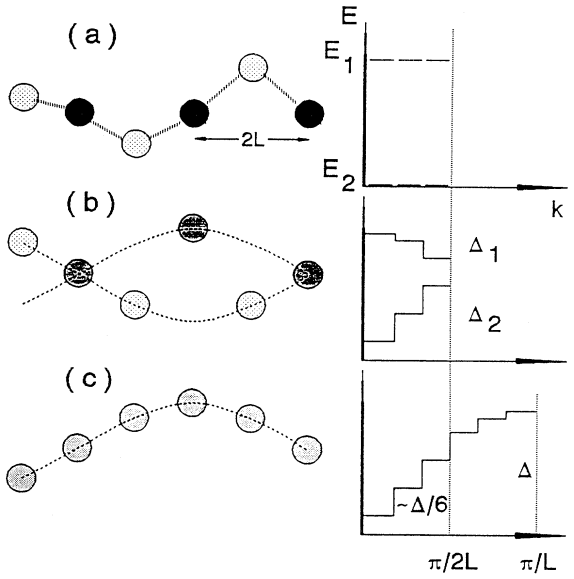

FIG. 2. Real-space oscillations and reciprocal-space energies for a finite linear chain of masses connected by springs of constant κ. [For clarity, transverse oscillations are shown, although longitudinal oscillations predominate in liquids.] (a) For alternating masses m_1 (grey) and $m_2=\infty$ (black), excitations consist of dispersionless, local oscillations, with energy $E_1=\hbar\sqrt{2\kappa/m_1}$. [Randomness would break the degeneracy of E_1, but excitations remain localized with an average energy-level spacing that is independent of domain size.] (b) Finite $m_2>m_1$ yields dispersive optical and acoustical branches, with bandwidths $\Delta_1=\hbar\{\sqrt{2\kappa(1/m_1+1/m_2)}-\sqrt{2\kappa/m_1}\}$ and $\Delta_2=\hbar\sqrt{2\kappa/m_2}$, respectively. (c) When $m_2=m_1=m$ the real-space primitive cell is reduced, leaving only an acoustical branch, with $\Delta=2\hbar\sqrt{\kappa/m}$. Bandwidths are independent of domain size, whereas the number of energy-levels, which fill Δ is proportional to s, yielding $|\delta E_s| \propto 1/s$.

Another contrast to the previous notion that slow response in glass-forming liquids comes from semirigid clusters (where activation over an intermediate barrier requires $\delta E>0$) is that we find $\delta E_s<0$. To show that $\delta E_s<0$ for all simple thermodynamic systems, consider a two-level system with energy-level spacing δE_2 [Fig. 4(a)] and relaxation governed by the master equations: $dN_0/dt=w_-N_1-w_+N_0$ and $dN_1/dt=w_+N_0-w_-N_1$. Assuming a symmetric intrinsic attempt frequency w_0, detailed balance yields $w_+=w_0e^{-\delta E_2/2k_BT}$ and $w_-=w_0e^{-(-\delta E_2)/2k_BT}$. The net relaxation rate for the out-of-equilibrium eigenstate is $w_2=w_++w_-=2w_0\cosh(\delta E_2/2k_BT)$.[42] Thus, simple systems with large energy-level spacing *always* relax faster than systems with small energy spacing. (The traditional result of slowly relaxing systems with large barriers requires three or more energy levels constrained to relax over an intermediate barrier [Fig. 4(b)], so that $w_3\sim 2/(w_+^{-1}+w_-^{-1})$.[42])

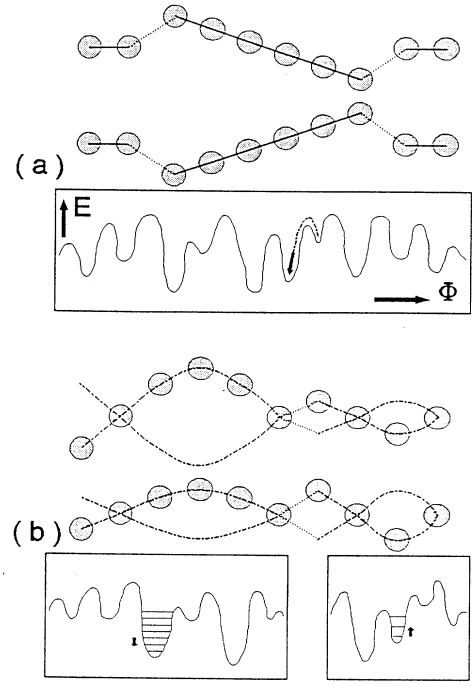

FIG. 3. Real-space and configuration-space comparison between response due to semirigid clusters and our model for localized normal modes. (a) Sudden repositioning of large semirigid clusters occurs via activation over a large energy barrier to a distant point in configuration space. This picture requires considerable inhomogeneity (rigid clusters held softly in place) and macroscopic ergodicity (if a single configuration space is to be defined for the entire sample). (b) DCD formation does not require structural inhomogeneity. Mesoscopic ergodicity may be characterized by a separate configuration space for each DCD. Primary response involves transitions between distinct energy-levels near a single minimum for each DCD. Secondary responses involving communication between domains (e.g., domain growth, direct energy exchange, or particle diffusion) have been shown to occur after primary response (Ref. 30).

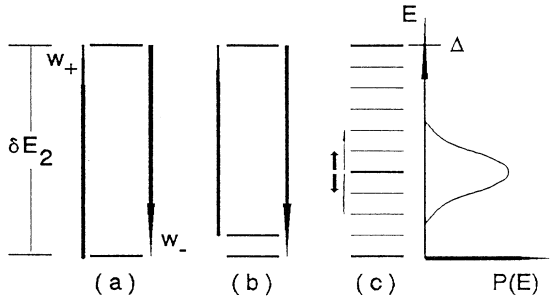

FIG. 4. (a) Two-level systems have net relaxation rates $[w_2=(w_+ +w_-)=2w_0\cosh(\delta E_2/2k_BT)]$ that increase with increasing energy spacing. (b) Three-level systems may have $w_3\sim 2/(w_+^{-1}+w_-^{-1})$ *only if* relaxation requires activation through an intermediate level (Ref. 42). (c) Multi-level systems (such as DCD's) involve multiple transitions between many levels. Near thermodynamic equilibrium, if transitions occur over a range of energy fluctuations ($P_{\delta E}$), net relaxation rates increase exponentially with increasing energy spacing.

Two-level systems have $w_2=w_0e^{|\delta E_2|/2k_BT}$ only if $|\delta E_2|\gg k_BT$. Multilevel systems (such as DCD's) may have transitions between many levels [Fig. 4(c)], so that the net relaxation rate varies exponentially with inverse size even if $|\delta E_s|\ll k_BT$. In general, thermal fluctuations combine closely spaced energy levels to form "super levels," with larger effective spacing. Specifically, assuming Gaussian fluctuations[36] in the energy of each level

$$\{P_{\delta E}\propto\exp[-(\delta E)^2sf''(E_e)/2k_BT]\}\ ,$$

and Fermi's Golden Rule for transitions that vary as the square of their overlap, the net relaxation rate may be written as

$$w_s\propto\int_{-\infty}^{+\infty}d(\delta E)P_{\delta E}^2e^{-\delta E/2k_BT}\propto e^{1/[16sf''(E_e)k_BT]}\ .$$

[Here $f(E)$ is the free energy per particle for the excitation of interest, and $f''(E_e)$ its curvature about equilibrium.] All glass-forming liquids we have analyzed have relaxation rates that increase exponentially with inverse size, indicting that primary response occurs near a stable equilibrium $[f''(E_e)>0]$, without activation over an intermediate barrier.

The final assumption is that randomness yields some specific domain-size distribution. Liquids (and other ergodic systems) generally exhibit a Gaussian distribution of domains, indicative of equilibrium long-ranged randomness.[24,25,28,43,44] For deviation σ about an average size $\bar{s}$, the distribution of DCD's is $n_s\propto e^{-[e(s-\bar{s})/\sigma]^2}$. Using $x=s/\sigma$, the net relaxation becomes

$$P(t)\propto P_0\int_0^{\infty}[xe^{-(x-\bar{x})^2}]e^{-tw_\infty e^{-c/x}}dx\ , \qquad (1)$$

where the "dynamical correlation coefficient" for thermally combined "super levels" is $C=-1/[16\sigma f''(E_e)k_Bt]$. The complex susceptibility as a function of frequency is equal to the Fourier transform of $-d[P(t)]/dt$. Using $w_x=w_\infty e^{-C/x}$, Eq. (1) yields

$$\chi(\omega)\propto P_0\int_0^{\infty}[xe^{-(x-\bar{x})^2}]\frac{1-i(\omega/w_x)}{1+(\omega/w_x)^2}dx\ . \qquad (2)$$

Equations (1) and (2) have four adjustable parameters: P_0 accommodates the magnitude of response, w_∞ governs the time scale of response, C adjusts the spectral shape, whereas the (scaled) average domain size $\bar{x}=\bar{s}/\sigma$ influences the magnitude, time scale, and spectrum of response.

COMPARISON WITH MEASUREMENTS

The size-dependent weight factor $[xn_x=x^{1-\theta}e^{-(x^\zeta-\bar{x})^2}]$ used in Eqs. (1) and (2) assumes homogeneous equilibrium response $(1-\theta=1)$ and a random distribution of domain *volumes* $(\zeta=1)$. If response was a surface effect, or if radius was the relevant parameter of randomness, then one would expect $1-\theta=2/3$ or $\zeta=1/3$, respectively. When fitting data that span sufficient dynamic range, these size-scaling exponents may be set free as additional adjustable parameters, so that size-scaling is solely established by the inverse-linear behavior in the exponent of $w_x=w_\infty e^{-C/x}$. From the dielectric response of salol and glycerol we obtain $1-\theta=0.98\pm0.13$ and $\zeta=0.994\pm0.04$. Excellent agreement with the exact predictions quantitatively confirms all assumptions of the model: homogenous equilibrium response $(1-\theta=1)$, Gaussian distribution of excitation *volumes* $(\zeta=1)$, *and* relaxation rates that vary exponentially with inverse size (otherwise $1-\theta$ and ζ would deviate to compensate). Empirically, within experimental uncertainty, Eq. (2) is the correct response function for these data.

In principle, both $\bar{x}$ and C could accommodate variations in the spectral shape of Eqs. (1) and (2). Experimentally, however, the ratio $\bar{x}/C$ $[=-16\bar{s}f''(E_e)k_BT]$ is constant, independent of temperature; for example, $\bar{x}/C=-0.182\pm0.003$ from the dielectric susceptibility of salol.[45] Furthermore, a similar ratio $(\bar{x}/C=-0.19\pm0.02)$ is found from a variety of measurements on other glass-forming liquids,[25,27] and $\bar{x}/C=0.197\pm0.02$ for magnetic relaxation in single-crystal iron;[24] but glycerol[7] is different $\bar{x}/C=-0.269\pm0.005$. Note, however, that the ratio of glycerol to salol is 1.48 ± 0.03, suggesting that most "liquids" have $D=3$ degrees of freedom, while glycerol has $D=2$. (Presumably hydrogen bonding reduces the degrees of freedom for elementary excitations in glycerol.) Combined, these measurements yield $\bar{x}|C|=(0.5415\pm0.007)/D$. Theoretically, such common behavior must be due to a ubiquitous mechanism for dynamical correlation.[46] Experimentally, once the constant value of $\bar{x}/C$ has been determined for a particular substance, Eqs. (1) and (2) accurately model observed behavior with a single adjustable parameter governing the entire shape of response.

The net primary response of a system can be determined by extrapolating Eq. (1) to $t=0$ or the real part of Eq. (2) to $\omega=0$. Figure 5 shows the temperature dependence of $1/\chi'(0)$ from measurements of salol and glycerol. The observed net response may be approximated

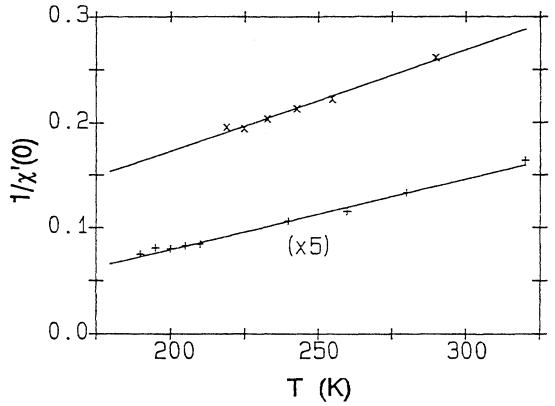

FIG. 5. Inverse net equilibrium response as a function of temperature for (×) salol (Ref. 47) and (+) glycerol (Ref. 7). Solid lines are the best fits to a Curie-Weiss law $[\chi'(0)=\Phi/(T-\theta)]$ yielding $\Phi=1040$ K and $\theta=21$ K for salol, and $\Phi=7500$ K and $\theta=82$ K for glycerol.

by the Curie-Weiss law $[\chi'(0)=\Phi/(T-\theta)$ solid lines], with $\Phi=1040$ K and $\theta=21$ K for salol, and $\Phi=7500$ K and $\theta=82$ K for glycerol.

Figure 6 is an Arrhenius plot of $\log_{10}(1/\nu_p)$ versus T_g/T, where T_g is the glass-transition temperature ($\sim$217 K for salol and $\sim$185 K for glycerol). In Fig. 6, so-called "strong"[2] (Arrhenius-like) liquids (e.g., SiO_2) exhibit linear behavior (solid line). Intermediate liquids (e.g., glycerol) show moderate deviations from Arrhenius-like behavior, which can be approximated by the VTF law (dashed curves).[7] "Fragile" liquids (e.g. salol) show very non-Arrhenius behavior, which is somewhat more poorly approximated by the VTF law.[47] For single exponential (Debye-like) response ($C=0$), the asymptotic relaxation rate corresponds to the peak frequency: $w_\infty=2\pi\nu_p$. For non-Debye response, ν_p depends on w_∞ and the width of the distribution, similar to the fact that $(1/\tau)\neq 2\pi\nu_p$ when $\beta\neq 1$ in the KWW function. For glass-forming liquids, $C<0$ so the largest

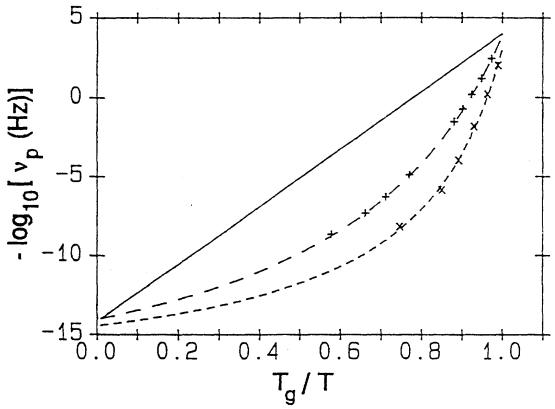

FIG. 6. Arrhenius plot of inverse peak-response frequency as a function of inverse reduced temperature. Solid line indicates Arrhenius-like behavior. The non-Arrhenius behavior of (×) salol (Ref. 47) and (+) glycerol (Ref. 7) may be approximated by the empirical VTF law, dashed curves.

DCD's relax the slowest: $w_\infty<2\pi\nu_p$. It is difficult to determine w_∞ accurately without careful analysis using Eq. (1) or (2), but typically $w_\infty/2\pi$ is on the low-frequency side of the absorption peak, where χ'' is an order of magnitude below its peak value. Since ν_p depends on w_∞ *and* the distribution of DCD sizes, no simple temperature dependence for ν_p can be found. Although w_∞ is a more fundamental relaxation rate, spectral widths are relatively weakly temperature dependent, so $1/w_\infty$ also diverges more rapidly than Arrhenius' law as temperature is lowered.

Intrinsic attempt frequencies should not vary significantly with temperature, suggesting that any significant change in the net relaxation rate must be due to the temperature dependence of $\bar{s}$ in $w_\infty=w_0e^{C/x_0}=w_0e^{-(D/0.5415)\bar{s}/s_0}$. Here w_0 is an intrinsic relaxation rate corresponding to a domain of size s_0. Presumably s_0 is the minimum number of particles which may form a DCD and relax coherently ($s_0\gtrsim 1$), but it is sufficient to assume that s_0 is some characteristic small size. Thus, slow relaxation of large domains comes from a rapid intrinsic attempt frequency, which is reduced by the virtually balanced net relaxation rate between closely spaced energy levels. This concept of rescaled relaxation rates is reminiscent of the model of Ngai and coworkers,[48,49] who assume that primary relaxation is *homogeneously* broadened by a coupling to low-energy excitations. In our approach, however, primary response is due directly to changes in the number of low-energy normal-modes; with the key distinction that we consider a *heterogeneous* distribution of exponentially relaxing domains.

Variations in $\bar{s}$ may be deduced from the measured net response normalized by the expected intrinsic response $\bar{s}\propto\chi'(0)/P_0$.[24] With decreasing temperature, Debye's T^3 law suggests that the intrinsic response of low-energy normal modes should *decreases* as $P_0\propto T^\gamma$, where $\gamma=3$. Experimentally, however, the net response *increases* as $\chi'(0)=\Phi/(T-\theta)$ (Fig. 5); hence the average DCD size must *increase* as

$$\bar{s}\propto\chi'(0)/P_0\propto[\Phi/(T-\theta)]/T^3 .$$

Indeed, least-squares fits to the data using $\ln(1/w_\infty)=a+b\chi'(0)/T^\gamma$ yield $\gamma=2.9\pm0.4$, quantitatively confirming the expected temperature dependence.

If changes in the observed relaxation rate are due solely to changes in DCD size, the model predicts a constant slope

$$B=(D/0.5415)\bar{s}(T_g)/s_0$$

in

$$[\ln(1/w_\infty)-\ln(1/w_0)]=B[\bar{s}(T)/\bar{s}(T_g)] .$$

Figure 7 is a semilog plot of $1/w_\infty$ as a function of reduced average DCD size,

$$\bar{s}(T)/\bar{s}(T_g)=[(T_g-\theta)T_g^3]/[(T-\theta)T^3] .$$

Salol exhibits a constant slope, with relatively rigid excitations ($B=38$ and $w_0=1.4\times10^{13}$ sec^{-1}, solid line).

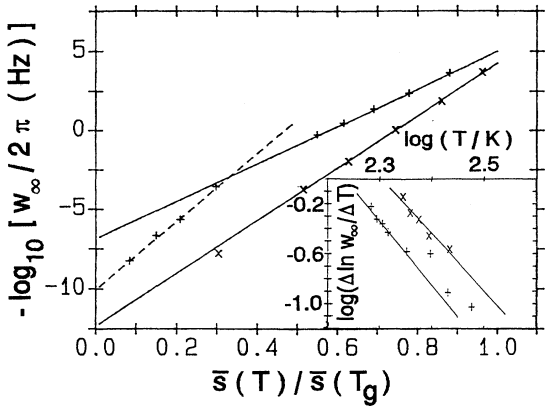

FIG. 7. Semilog plot of inverse asymptotic relaxation rate as a function of $\bar{s}(T)/\bar{s}(T_g)=[(T_g-\theta)T_g^3]/[(T-\theta)T^3]$. The model predicts constant slope (B) in $[\ln(1/w_\infty)-\ln(1/w_0)] = B[\bar{s}(T)/\bar{s}(T_g)]$. Both ($\times$) salol (Ref. 46) and (+) glycerol (Ref. 7) exhibit regions of linear behavior, indicating that net response may be characterized by temperature dependent $\bar{s}$, and a constant microscopic relaxation rate: $w_0=1.4\times10^{13}$ sec^{-1} in salol (solid line), and $w_0=5\times10^7$ sec^{-1} for $T<240$ K (solid line) and $w_0=7\times10^{10}$ sec^{-1} for $T\geq240$ K (dashed line) in glycerol. Inset: log-log plot of $\Delta\ln(w_\infty)/\Delta T$ vs T. Over the available temperature range, the slope is -4.9 ± 0.4, consistent with $\Delta\ln(w_\infty)/\Delta T\ (\propto 1/T^5)$ expected from the model.

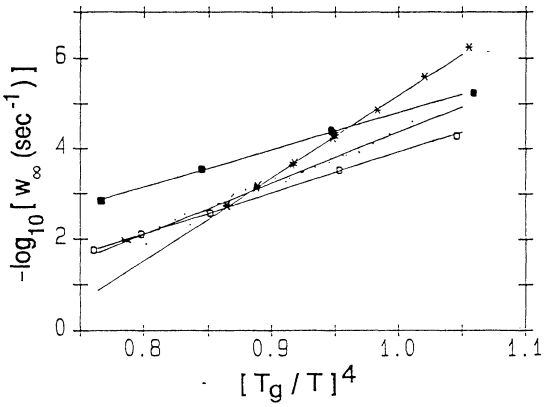

FIG. 8. Semi-log plot of inverse asymptotic relaxation rate as a function of $[T_g/T]^4$ for ● AgI-Ag_2So_4-Ag_2WO_4 (Ref. 57), * phenolphthalein (Ref. 28), ○ Se_{84}-As_{12}-Ge_4 and ● Se_{47}-As_{46}-Ge_7 (Ref. 18). Over a broad temperature range, the model predicts $[\ln(1/w_\infty)-\ln(1/w_0)]\propto 1/T^4$. All systems show constant slope, with intercepts that yield intrinsic relaxation rates of $w_0=10^3$–10^{13} sec^{-1}; see Table I.

This intrinsic relaxation rate coincides with the observed microscopic band at $w_0/2\pi\simeq1$ THz.[50] Glycerol has two regimes of constant slope. A low-temperature regime ($T<240$ K) of relatively soft excitations ($w_0=5\times10^7$ sec^{-1} with $B=27$, solid line), and a high-temperature regime of stiffer excitations ($w_0=7\times10^{10}$ sec^{-1} with $B=49$, dashed line). At low temperatures, w_0 is characteristic of measured rotational jump frequencies, $\sim10^7$ sec^{-1}.[51] At higher temperatures, w_0 is consistent with local relaxation rates, $\sim10^{11}$ sec^{-1}.[52] Since $B\propto D/s_0$, a change in slope could be due to a change in the degrees of freedom for the primary excitations or a change in the minimum size for coherent relaxation. For $T\leq240$ K we find $\bar{x}/|C|=(0.269\pm0.005)=0.5415/D$, whereas for $T\geq240$ K, $\bar{x}/|C|=0.29\pm0.07$; evidently, the increased slope above 240 K is primarily due to a sharp decrease in s_0.

Sometimes it is inconvenient (or impossible) to accurately determine the net response of a sample. Fortunately, in liquids where $T>T_g\gg\theta$, the Curie-Weiss law may be approximated by the Curie law, $\chi'(0)\approx\Phi/T$. If, in addition, the temperature is still low enough that Debye's T^3 law remains valid, the model predicts relaxation rates that vary as $[\ln(1/w_\infty)-\ln(1/w_0)]\propto1/T^4$. Indeed, a log-log plot of $\Delta\ln(w_\infty)/\Delta(\propto1/T^5)$ (inset of Fig. 7) shows a slope of -4.9 ± 0.4 for both salol and glycerol. Figure 8 is a semilog plot of $1/w_\infty$ as a function of $(T_g/T)^4$ for several glass-forming liquids. All data are consistent with $\bar{s}\propto1/T^4$ predicted by the model, but these measurements are over too limited a range to show deviations from Arrhenius' law $[\ln(1/\nu_p)-\ln(1/\nu_0)]\propto1/T$. Assuming Arrhenius behavior, however, generally yields nonphysical attempt frequencies ($\nu_0\gg10^{20}$ Hz), whereas Table I shows more reasonable values for w_0.

Statistical comparison between the temperature dependence predicted by the model $[\ln(1/w_\infty)-\ln(1/w_0)]\propto\chi'(0)/T^3$ and the VTF law $[\ln(1/\nu_p)-\ln(1/\nu_0)]\propto1/(T-T_0)$ is hampered by the model's relevance to the asymptotic relaxation rate, which is not as well defined *experimentally* as the peak-absorption frequency. Nevertheless, χ^2 deviations of w_∞ from the model, are comparable to deviations of ν_p from the VTF law: $\chi^2/\chi^2_{\mathrm{VTF}}=0.39$ and 3.7 for salol and glycerol, respectively. Although T_0 is often suggestively close to the Kauzmann temperature (T_k),[53] many measurements indicate physically unreasonable $T_0<T_k$.[45] The model provides equally good agreement with the data, without invoking this additional adjustable parameter; evidently T_0 is superfluous, with no physical significance, and ν_p is an artifice of the intrinsic relaxation rate and a most probable domain size.

Once the intrinsic relaxation rate and temperature-dependent net response of a particular substance have been determined, Eqs. (1) and (2) describe observed behavior with only the single adjustable parameter that governs the spectrum of response. For example, Eq. (2) may be rewritten

$$\chi(\omega)=\frac{\Phi}{T-\Theta}\,\frac{\int_0^\infty(xe^{-(x-\bar{x})^2})\{[1-i(\omega/W_x)]/[1+(\omega/W_x)^2]\}dx}{\int_0^\infty[xe^{-(x-\bar{x})^2}]dx}\,, \tag{3}$$

TABLE I. Fitting parameters for various glass-forming liquids. ν_0 is the apparent attempt frequency, assuming the VTF law for salol and glycerol, and Arrhenius' law for the other substances. w_0 is the intrinsic relaxation rate, and B the slope, in the model expression $[\ln(1/w_\infty)-\ln(1/w_0)]=B[\bar{s}(T)/\bar{s}(T_g)]$, assuming $[\bar{s}(T)/\bar{s}(T_g)]=[(T_g-\theta)T_g^3/(T-\theta)T^3]$ for salol and glycerol, and $=[(T_g/T)^4]$ for the other substances. D is the apparent degrees of freedom for the elementary excitations. Also shown are the Curie (Φ) and Weiss (θ) constants for the dielectric response of salol and glycerol.

Ref.	ν_0 (Hz)	Liquid		w_0 (sec^{-1})	B	D	$\Phi(K)$	$\theta(K)$
45	3×10^{14}	Salol		1.4×10^{13}	38	3	1040	21
7	4×10^{15}	Glycerol	<240 K	5×10^{7}	27	2	7500	82
			≥240 K	7×10^{10}	49			
28	10^{68}	Phenolphthalein		1×10^{13}	42	3		
18	10^{30}	Se_{84}-As_{12}-Ge_4		3×10^{3}	19	3		
	10^{25}	Se_{47}-As_{46}-Ge_7		1×10^{5}	21	3		
57	10^{48}	AgI-Ag_2SO_4-Ag_2WO_4		8×10^{6}	26	3		

where $\bar{x}=|C|(0.5415/D)$ and

$$w_x=w_0e^{-B[\bar{s}(T)/\bar{s}(T_g)]}e^{-C/x}.$$

Using the values in Table I, and C as the only adjustable parameter, Fig. 9 shows excellent agreement with measured dielectric absorption of salol and glycerol over a wide temperature range, and more than 13 orders of magnitude in frequency. The magnitude of C (inset) exhibits a maximum at a temperature (T_C) about 50 K above T_g.

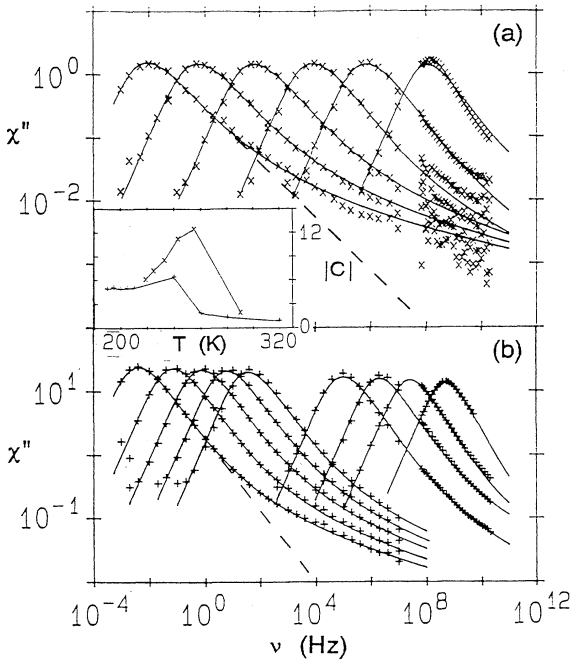

FIG. 9. Log-log plot of dielectric absorption as a function of frequency for (a) salol (Ref. 45) and (b) glycerol (Ref. 7). At high frequencies, the data demonstrate unambiguous deviation from the empirical KWW stretched-exponential [frequency-dependent form of $e^{-(t/\tau)^\beta}$, dashed lines]. Solid curves are the best fits to Eq. (3), using values from Table I, and C as the only adjustable parameter. Inset: the magnitude of the dynamical-correlation coefficient for both (×) salol and (+) glycerol exhibits a peak at temperature $T_C=T_g+(\sim50$ K), and rapid decrease above T_C.

Presumably, the maximum in $|C|$ indicates an optimal balance between thermal energy (which drives dynamical correlation) and entropy (which drives randomness). Above T_C, correlations drop rapidly as entropy prevails.

The behavior near T_C signifies abrupt changes in the spectrum of response, which may be related to the dynamical anomalies reported for various glass-forming liquids at 35–90 K above T_g.[54,55] An ergodicity-breaking transition above T_g was predicted by mode-coupling theory (MCT),[56] but we emphasize that our model of exponentially relaxing domains is incongruent with MCT. It is possible that MCT could be relevant to the interactions between DCD's (indeed, in Fig. 7, the change in w_0 of glycerol suggests intermolecular rotations below T_C, and intramolecular relaxations above T_C), but it is not clear how MCT could explain the correct distribution of *exponentially relaxing* domains. Even for glycerol at $T>T_C$ (≥240 K, where the diminished dynamic range of the data increases the uncertainty), we find $1-\theta=0.6\pm0.5$ and $\zeta=1.06\pm0.07$, affirming all assumptions of our model. Furthermore, using our model, there is clear evidence for a *well-defined* ergodicity breaking transition at $T_e=T_g$.[28]

CONCLUSIONS

A thermodynamic model for a Gaussian distribution of independently relaxing domains gives excellent agreement with observed dielectric susceptibility of salol and glycerol over more than 13 orders of magnitude in frequency. The quality and range of these data permit quantitative confirmation of all assumptions of the model. As a function of temperature, the model predicts that observed relaxation rates should vary as $[\ln(1/w_\infty)-\ln(1/w_0)]\propto\bar{s}$. Changes in the average domain size may be deduced from the measured net response normalized by the expected intrinsic response, $\bar{s}\propto\chi'(0)/T^3$. Over a broad temperature range above T_g, $\bar{s}\propto1/T^4$. In contrast to the Arrhenius law ($\sim1/T$), the model yields excellent agreement with observed relaxation rates, *and* physically meaningful values for w_0, without resorting to the three adjustable parameters of the VTF law. Thus, non-Arrhenius response may be characterized by temperature-dependent dynamically

correlated domain size, and a *constant* intrinsic relaxation rate.

ACKNOWLEDGMENTS

I thank R. Böhmer, N. A. Clark, P. K. Dixon, G. Li, R. Malzbender, N. Menon, S. R. Nagel, B. Pouligny, and E. Sanchez for their original data. Enlightening conversations with C. A. Angell, R. Böhmer, N. A. Clark, M. A. Glaser, S. M. Lindsay, W-L. Luo, R. F. Marzke, P. F. McMillan, W. F. Oliver, N. J. Tao, M. R. Scheinfein, M. F. Shlesinger, and G. H. Wolf are gratefully acknowledged. It is also a pleasure to thank R. Böhmer and A. Loidl for their hospitality, and the Sonderforschungsbereich 262 for support, during final preparation of this manuscript at the Technische Hochschule in Darmstadt Germany.

[1]S. Arrhenius, Z. Phys. Chem. **4**, 226 (1889).

[2]C. A. Angell, J. Non-Cryst. Solids **131-133**, 13 (1991).

[3]H. Vogel, Phys. Z **22**, 645 (1921).

[4]G. Tammann and W. Hesse, Z. Anorg. Allg. Chem. **156**, 245 (1926).

[5]G. S. Fulcher, J. Am. Ceram. Soc. **8**, 339 (1925).

[6]P. W. Anderson, in *Ill-Condensed Matter,* edited by R. Balian, R. Maynard, and G. Toulouse (North-Holland, Amsterdam, 1979), p. 159.

[7]N. Menson, K. P. O'Brien, P. K. Dixon, L. Wu, S. R. Nagel, B. D. Williams, and J. P. Carini, J. Non-Cryst. Solids **141**, 61 (1992).

[8]R. G. Palmer, D. L. Stein, E. Abrahams, and P.W. Anderson, Phys. Rev. Lett. **53**, 958 (1984).

[9]J. T. Bendler and M. F. Shlesinger, J. Stat. Phys. **53**, 531 (1988).

[10]H. Bässler, Phys. Rev. Lett. **58**, 767 (1987).

[11]J. Souletie and D. Bertrand, J. Phys. (Paris) I **1**, 1627 (1991).

[12]A. K. Doolittle, J. Appl. Phys. **22**, 1471 (1951).

[13]M. L. Williams, R. F. Landel, and D. J. Ferry, J. Am. Chem. Soc. **77**, 3701 (1955).

[14]M. H. Cohen and G. S. Grest, Phys. Rev. B **20**, 1077 (1979).

[15]G. Adams and J. H. Gibbs, J. Chem. Phys. **43**, 139 (1965).

[16]R. Zwanzig, J. Chem. Phys. **79**, 4507 (1983).

[17]B. Madan, T. Keyes, and G. Seeley, J. Chem. Phys. **94**, 6762 (1991).

[18]R. Böhmer and C. A. Angell, Phys. Rev. B **45**, 10091 (1992).

[19]H. J. Queisser, Appl. Phys. A **52**, 261 (1991).

[20]H. Scher, M. F. Shlesinger, and J. T. Bendler, Physics Today, **41**, 26 (1991).

[21]J. Klafter and M. F. Shlesinger, Proc. Natl. Acad. Sci. USA, **83**, 848 (1986).

[22]R. V. Chamberlin and D. N. Haines, Phy. Rev. Lett. **65**, 2197 (1990).

[23]R. V. Chamberlin and F. Holtzberg, Phys. Rev. Lett. **67**, 1606 (1991).

[24]R. V. Chamberlin and M. R. Scheinfein, Science **260**, 1098 (1993).

[25]R. V. Chamberlin and M. R. Scheinfein, Ultramicrosc. **47**, 408 (1992).

[26]J. Zhang, J. F. Ma, S. E. Nagler, and S. E. Brown, Phys. Rev. Lett. **70**, 3095 (1993).

[27]R. V. Chamberlin, D. N. Haines, and D. W. Kingsbury, J. Non-Cryst. Solids **131-133**, 192 (1991).

[28]R. V. Chamberlin, R. Böhmer, E. Sanchez, and C. A. Angell, Phys. Rev. B **46**, 5787 (1992).

[29]W. E. Moerner, in *Persistent Spectral Hole-Burning: Science and Applications,* edited by W. E. Moerner (Springer-Verlag, Berlin, 1988), p. 1.

[30]K. Schmidt-Rohr and H. W. Spiess, Phys. Rev. Lett. **66**, 3020 (1991); and K. Schmidt-Rohr (private communication).

[31]K. Schmidt-Rohr, J. Clauss, and H. W. Spiess, Macromolecules, **25**, 3273 (1992).

[32]P. Choquard and J. Clerouin, Phys. Rev. Lett. **50**, 2086 (1983).

[33]Y. Hiwatari, H. Miyagawa, and T. Odagaki, Solid State Ionics **47**, 179 (1991), and references therein.

[34]J-L. Barrat and M. L. Klein, Annu. Rev. Phys. Chem. **42**, 23 (1991).

[35]B. Pouligny, R. Malzbender, P. Ryan, and N. A. Clark, Phys. Rev. B **42**, 988 (1990); and N. A. Clark and M. A. Glaser (private communication).

[36]R. Kubo, K. Matsuo, and K. Kitahara, J. Stat. Phys. **9**, 51 (1973).

[37]W. P. Halperin, Rev. Mod. Phys. **58**, 533 (1986).

[38]H. Fröhlich, Physica **4**, 406 (1937).

[39]R. Kubo, J. Phys. Soc. Jpn. **17**, 975 (1962).

[40]C. Kittel, *Introduction to Solid State Physics,* 5th ed. (Wiley, New York, 1976).

[41]R. G. Palmer and D. L. Stein, in *Relaxations in Complex Systems,* edited by K. L. Ngai and G. B. Wright (National Technical Information Service, Springfield VA, 1984), p. 253.

[42]J. C. Gill, Rep. Prog. Phys. **38**, 91 (1975).

[43]J. H. Gibbs, B. Bagchi, and U. Mohanty, Phys. Rev. B **24**, 2893 (1981).

[44]S. Chekmarev, Chem. Phys. Lett. **120**, 531 (1985).

[45]P. K. Dixon, L. Wu, S. R. Nagel, B. D. Williams, and J. P. Carini, Phys. Rev. Lett. **65**, 1108 (1990).

[46]The mechanism could involve the Riemann zeta function, since $\zeta(4)=\Sigma_{j=1}^{\infty}(1/j)^4=\pi^4/90=2(0.5412)$, and $\zeta(4)$ occurs commonly in condensed matter physics. One example is the Van der Waals interaction summed over a sequence of spherical shells with radii $r_j=jr_0$: $\sum_{j=1}^{\infty}[\int d\Omega_j(r_j)^{-6}]\propto\zeta(4)$. Another example is the Debye model for the energy of Boson-like waves at low temperatures: $\int_0^{\infty}dE(E)^3(e^{E/k_BT}-1)^{-1}=\int_0^{\infty}dE(E)^3[\sum_{j=1}^{\infty}e^{-jE/k_BT}]=6\sum_{j=1}^{\infty}(k_BT/j)^4=6(k_BT)^4\zeta(4)$.

[47]P. K. Dixon, Phys. Rev. B **42**, 8179 (1990).

[48]K. L. Ngai, J. Non-Cryst. Solids **131-133**, 80 (1991).

[49]K. L. Ngai, R. W. Rendell, A. K. Rajagopal, and S. Teitler, Ann. N.Y. Acad. Sci. **484**, 150 (1986).

[50]G. Li, W. M. Du, A. Sakai, and H. Z. Cummins, Phys. Rev. A **46**, 3343 (1992).

[51]M. Elwenspoek, M. Soltwisch, and D. Quitmann, Mol. Phys. **35**, 1221 (1978).

[52]F. Fujara, W. Petry, R. M. Diehl, W. Schnauss, and H. Sillescu, Europhys. Lett. **14**, 563 (1991).

[53]W. Kauzmann, Chem. Rev. **43**, 219 (1948).

[54]B. Frick, B. Farago, and D. Richter, Phys. Rev. Lett. **64**, 2921 (1990).

[55]M. Elmroth, L. Börjesson, and L. M. Torell, Phys. Rev. Lett. **68**, 79 (1992).

[56]W. Götze and L. Sjögren, Rep. Prog. Phys. **55**, 241 (1992).

[57]R. Böhmer, H. Senapati, and C. A. Angell, J. Non-Cryst. Solids **131-133**, 192 (1991).